Original Article

MOLECULAR METABOLISM

Programmed increases in LXRα induced by paternal alcohol use enhance offspring metabolic adaptation to high-fat diet induced obesity

Richard C. Chang, Kara N. Thomas, Yudhishtar S. Bedi, Michael C. Golding*

ABSTRACT

Objectives: Paternally inherited alterations in epigenetic programming are emerging as relevant factors in numerous disease states, including the growth and metabolic defects observed in fetal alcohol spectrum disorders. In rodents, chronic paternal alcohol use induces fetal growth restriction, as well as sex-specific alterations in insulin signaling and lipid homeostasis in the offspring. Based on previous studies, we hypothesized that the observed metabolic irregularities are the consequence of paternally inherited alterations liver x receptor (LXR) activity.
Methods: Male offspring of alcohol-exposed sires were challenged with a high-fat diet and the molecular pathways controlling glucose and lipid homeostasis assayed for LXR-induced alterations.
Results: Similar to findings in studies employing LXR agonists we found that the male offspring of alcohol-exposed sires display resistance to diet-induced obesity and improved glucose homeostasis when challenged with a high-fat diet. This improved metabolic adaptation is mediated by LXRα trans-repression of inflammatory cytokines, releasing IKKβ inhibition of the insulin signaling pathway. Interestingly, paternally programmed increases in LXRα expression are liver-specific and do not manifest in the pancreas or visceral fat.
Conclusions: These studies identify LXRα as a key mediator of the long-term metabolic alterations induced by preconception paternal alcohol use.

Keywords Epigenetic programming; Liver X receptor; Nuclear receptor; Insulin signaling; Inflammation; Paternal alcohol exposure; Metabolic programming; Preconception; Developmental origins of adult disease

1. INTRODUCTION

Despite clear evidence that parental histories of drug abuse, overnutrition, malnutrition, social stress, and environmental exposures influence fetal development, the long-term contributions of preconception history to the development of disease remain a significant gap in our understanding of developmental toxicology [1,2]. This is especially true of paternal preconception exposures, which are a largely ignored aspect of patient history and are dramatically underexplored in relevant biomedical models. Indeed, although maternal exposures to alcohol, cigarettes, and other drugs of abuse have well-established effects on fetal development, the importance of the lifestyle choices of the father have only recently been recognized for their potential to influence offspring health [3]. However, the molecular pathways by which preconception paternal drug exposures exert a long-term influence on offspring growth and development remain poorly defined.
Similar to rodent models examining a wide range of other environmental and metabolic stressors, paternal exposures to alcohol and drugs correlate with alterations to the sperm epigenome, as well as changes in offspring behavior, metabolism and the propensity to develop disease [3,4]. Using a mouse model of voluntary consumption, our lab recently identified an association between chronic paternal alcohol use and long-term effects on the growth and metabolic health of the offspring [5–7]. Specifically, the offspring of males continuously exposed to alcohol before conception displayed placental dysfunction and late-term fetal growth restriction [5,6]. Interestingly, the male offspring of alcohol-exposed fathers continued to exhibit growth deficits in postnatal life, which persisted into adolescence [7]. Similar to our studies, Rompala and colleagues have also described alcohol-induced effects on the postnatal growth of male offspring using an inhalation model of alcohol exposure [8]. However, the molecular basis of these growth defects remains unknown.
In our model, the long-term growth restriction identified in the male offspring associated with heightened insulin sensitivity, increased markers of hepatic fibrosis, suppressed cytokine profiles within the liver, and upregulation of genes in the liver x/retinoid x/farnesoid x receptor pathways [7]. Previously, male-inherited alterations in the expression of liver x receptor alpha (LXRα) were described in a mouse

Department of Veterinary Physiology & Pharmacology, College of Veterinary Medicine and Biomedical Sciences, Texas A&M University, College Station, TX, 77843, USA

*Corresponding author. 4466 TAMU, College of Veterinary Medicine and Biomedical Sciences, Texas A&M University, College Station, TX, 77843-4466, USA. E-mail: mgolding@cvm.tamu.edu (M.C. Golding).

Received August 8, 2019 • Revision received September 25, 2019 • Accepted September 29, 2019 • Available online 3 October 2019

https://doi.org/10.1016/j.molmet.2019.09.016

Abbreviations

LXRα	liver x receptor alpha
LXRβ	liver x receptor beta
RXRα	retinoid receptor alpha
FXR	farnesoid receptor
CD	standard chow diet
HFD	high-fat diet
NFkB	nuclear factor k B
TNFα	tumor necrosis factor alpha
IL1β	interleukin 1 beta
IL*6*	interleukin 6
TLR	toll-like receptor
Ikkβ	inhibitor of nuclear factor k B Kinase β
IRS1	Insulin receptor substrate 1
AKT	serine/threonine kinase 1
PEPCK	phosphoenolpyruvate carboxykinase
G6PC	glucose-6-phosphatase catalytic subunit
Untr6	untranscribed region of chromosome 6
FASN	fatty acid synthase
SREBF1	sterol regulatory element binding transcription factor 1
Apoa5	apolipoprotein A5
TGF-β	transforming growth factor beta
Timp1	tissue inhibitor of metalloproteinases 1
Smad2	mothers against decapentaplegic homolog 2
Col4a1	collagen subtype 4a1
Col5a2	collagen subtype 5a2
Col6a2	collagen subtype 6a2

model of intrauterine growth restriction (IUGR) induced by late-term maternal malnutrition [9]. Here, multigenerational, paternally programed repression of hepatic LXRα expression induced glucose intolerance and the misregulation of lipogenic genes in liver [9]. However, in contrast to the effects propagated through IUGR males, the male offspring of alcohol-exposed fathers displayed an up-regulation of LXR stimulated pathways [7].

Liver X receptors regulate numerous aspects of cholesterol, fatty acid, and glucose homeostasis, and have well-defined roles in controlling immune function and neurodevelopment [10]. Therefore, this nuclear receptor family may represent a mechanistic hub mediating male-inherited alterations in metabolic phenotypes and could be linked to the wide variations and sex-specific outcomes observed across multiple models of altered developmental programming. In previous studies, treatment with LXR agonists suppressed activation of glycogenic pathways in the liver and protected mice from diet-induced obesity [11–13]. Based on these observations, we hypothesized that the male offspring of alcohol-exposed sires would exhibit programmed resistance to diet-induced obesity and improved metabolic adaptation to a high-fat diet. Therefore, we set out to test this assertion and define the molecular mechanisms by which paternally-programmed increases in LXR activation influence the regulation of glucose homeostasis in the offspring of males chronically exposed to alcohol.

2. MATERIALS AND METHODS

2.1. Animal work

All experiments were conducted under AUP 2017-0308 and approved by the Texas A&M University IACUC. This study utilized C57BL/6J mice (RRID:IMSR_JAX:000664), which were obtained from and housed in the Texas A&M Institute for Genomic Medicine and maintained on a 12-hour light/dark cycle.

2.2. Preconception paternal alcohol exposures

We maintained individually caged postnatal day 90 adult males on a standard diet (catalog no. 2019, Teklad Diets, Madison, WI, USA) and exposed them to either a control or alcohol preconception treatment using a previously described limited access model of voluntary exposure [5–7]. In this model, males are provided limited access to the preconception treatments during a four-hour window, beginning one hour after the initiation of the dark cycle. Specifically, we provided experimental males access to a solution of 10% (w/v) ethanol (catalog no. E7023; Millipore-Sigma, St. Louis, MO, USA) and 0.066% (w/v) Sweet'N Low (Cumberland Packing Corp, Brooklyn NY, USA), while control males received a solution of 0.066% (w/v) Sweet'N Low alone. At the conclusion of each four hour period, we recorded the amount of fluid consumed by each male mouse and weighed the males on a weekly basis.

After a 70-day preconception treatment period, corresponding to the approximate length of two spermatogenic cycles, we placed two naturally cycling females into a new cage along with each exposed male. During the matings, we did not give the males access to the alcohol or control preconception treatments. After six hours, we confirmed matings by the presence of a vaginal plug and returned both the male and female mice to their original cages. We rested males for 72-hours, where the preconception exposure was resumed, and then used them again in a subsequent mating. We repeated this procedure until we obtained the requisite number of pregnancies.

2.3. Postnatal dietary treatments

We subjected dams to minimal handling, maintained them on a Breeder diet (catalog no. 5058; LabDiet, St. Louis, MO, USA), and monitored them for delivery twice daily. After weaning, we randomly separated male littermates sired by control and alcohol-exposed males into two treatment groups, with three males, each derived from different sire x dam pairings, co-housed in a single cage. We maintained the male offspring on a standard diet (catalog no. 2019, Teklad Diets, Madison, WI, USA) until 8-weeks of age. After 8 weeks, one group continued to receive the standard chow diet (CD – catalog no. 2019, Teklad Diets, Madison, WI, USA), while we fed the other a high-fat diet, with 60% kcal derived from fat (HFD – catalog no. D12492; Research Diet Inc., New Brunswick, NJ, USA). To monitor the progress of diet-induced obesity, the body weight gain and food intake of each group of males was measured weekly. At 20 weeks of age, mice were fasted overnight, terminated and both physiological fluids and tissues collected.

2.4. Insulin and glucose tolerance tests

At 6 and 12 weeks of age, we fasted the male offspring of alcohol-exposed and control sires overnight and assayed differences in glucose and insulin tolerance, with a minimum of one-week recovery time between these separate tests. Here, we injected mice with a single intraperitoneal injection of either D-glucose (2 g/kg body weight; catalog no. SG8270; Millipore-Sigma, St. Louis, MO, USA) or insulin (1 unit/kg body weight; catalog no. 89508-914; VWR, Radnor, PA, USA) and measured blood glucose levels using Clarity Plus - Blood Glucose Test Strips (catalog no. DTG-GL5PLUS; Clarity Diagnostics, Boca Raton, Florida, USA) from 5ul of blood drawn from the tail vein. For glucose tolerance tests, we measured blood glucose levels at 0, 30, 60, 90,

120, 150, and 180 min post-injection. For insulin tolerance tests, we measured blood glucose levels at 0, 15, 30, 45, 60, 120, and 180 min after insulin injection. Each experimental group contains six males ($n = 6$).

2.5. Liver perfusion assay

When mice were twenty weeks of age, we randomly selected six males from each treatment group to evaluate insulin signaling by quantifying levels of IRS1 (Ser307) and AKT (Ser473) phosphorylation in the liver. We fasted mice for 12 h and then anesthetized them with 2% isoflurane [14], until the animals achieved a deep plane of anesthesia, demonstrating a lack of a righting reflex and a ~50% reduction in respiratory rate. At this point, we opened the body cavity of the mouse and perfused the liver with either 37 °C PBS + 0.1% BSA (Control) or 2 units/kg of an insulin solution (10 nM insulin, Sigma, in PBS + 0.1% BSA; catalog no. 89508-914; VWR, Radnor, PA, USA) at a flow rate of 100 ml/h. During this procedure, we clamped the suprahepatic vessel and inserted a 27-gauge syringe into the intrahepatic cava. After observing liver perfusion, we cut the hepatic portal vein open. Throughout the procedure, we kept a nose cone containing gauze soaked in isoflurane over the nose of the animal and only removed it when the rate of respiration dipped down below 25%. After five minutes, we euthanized the animals by cervical dislocation and collected tissues of interest, including liver, kidney, and pancreas, which were snap-frozen in liquid nitrogen. Each experimental group contains six different animals ($n = 6$).

2.6. Western immunoblot analysis

Liver tissue samples were collected and homogenized in a Tris lysis buffer including 50 mM Tris, 1 mM EGTA, 150 mM NaCl, 1% Triton X-100, 1% β-mercaptoethanol, 50 mM NaF, 1 mM Na3VO4; at pH 7.5. 20 μg of protein was separated on 10% sodium dodecyl sulfate—polyacrylamide gels and transferred to nitrocellulose membranes. The primary antibodies used in this study were as follows: anti-phosphorylated protein kinase B (AKT) at Serine 473 (catalog no. 700392; RRID:AB_2532320; Thermo-Fisher, Waltham, MA, USA), anti-AKT (catalog no. 44609G; RRID:AB_2533692; Thermo-Fisher, Waltham, MA, USA) anti-phosphorylated Inhibitor Of Nuclear Factor Kappa B Kinase Subunit Beta (IKK beta) at Tyrosine 199 (catalog no. ab59195; RRID:AB_943810; Abcam, Cambridge, MA, USA), anti-IKK beta (catalog no. ab124957; RRID:AB_10975710; Abcam, Cambridge, MA, USA), anti-phosphorylated Insulin receptor substrate 1 (IRS1) at Serine 307 (catalog no. ab5599; Abcam, Cambridge, MA, USA; RRID:AB_304975), anti-LXRα (catalog no. ab41902; RRID:AB_304975; Abcam, Cambridge, MA, USA) and anti-beta actin (catalog no. ab49900; RRID:AB_867494; Abcam, Cambridge, MA, USA). Blots were visualized by using secondary antibodies conjugated to horseradish peroxidase (catalog no. sc-2004; RRID:AB_631746; Santa Cruz Biotechnology, Santa Cruz, CA, USA) and an enhanced chemiluminescence detection system (Pierce, Rockford, IL, USA). Relative AKT phosphorylation was derived as a ratio to total AKT, relative IKK beta phosphorylation was derived as a ratio to total IKK beta, and relative IRS1 phosphorylation was derived as a ratio to beta actin. Band intensities were quantified by densitometry using ImageJ (RRID:SCR_003070; National Institutes of Health, Bethesda, MD, USA). Each experimental group contains protein extracts derived from six to eight different animals ($n = 6–8$).

2.7. Measurement of physiological parameters

We measured male plasma alcohol concentrations using an Ethanol Assay Kit (catalog no. ECET100; BioAssay Systems, Hayward, CA, USA) according to manufacturer's protocol. We determined plasma insulin levels post-mortem using the Mouse Insulin ELISA kit (catalog no. EMINS; Thermo-Fisher, Waltham, MA, USA), according to the recommended protocol. We measured levels of IL1B, IL6, and TNFα using commercial ELISA assays (catalog no. KMC0061 and KMC0011; Thermo-Fisher, Waltham, MA, USA and catalog mo. Ab100689 and Ab100747; Abcam, Cambridge, MA, USA). To determine total cholesterol levels, we used the Total Cholesterol Assay Kit (catalog no. STA- 384; Cell Biolab, Inc, San Diego, CA USA), according to the recommended protocol. To compare the levels of low-density and high-density lipoproteins, we used a colorimetric Cholesterol Assay Kit (catalog no. ab65390; Abcam, Cambridge, MA, USA), according to the recommended protocol. We used the Triglyceride Assay Kit (catalog no. ab65336; Abcam, Cambridge, MA, USA) to contrast the abundance of hepatic triglycerides, according to the suggested protocol. To compare the levels of hydroxyproline, we used the Hydroxyproline Assay Kit (catalog no. MAK008; Millipore-Sigma, St. Louis, MO, USA), and followed the recommended protocol.

2.8. RNA isolation and RT-qPCR analysis of gene expression

Total RNA was isolated from 20-week-old liver, pancreas and visceral fat using an RNeasy Plus Mini Kit, (catalog no. 74134; Qiagen, Germantown MD, USA) according to manufacturer's instructions. One microgram of purified total RNA was treated with amplification grade DNase I (catalog no. AMPD1; Millipore-Sigma, St. Louis, MO, USA) according to the manufacturer's recommendations and seeded into a reverse transcription reaction using the High Capacity cDNA Reverse Transcription Kit (catalog no. 4368814; Thermo-Fisher, Waltham, MA, USA), where the reaction mixture was brought to 25 °C for 10 min, 37 °C for 120 min, and then 70 °C for 5 min. Relative levels of candidate gene transcripts were analyzed using the Dynamo Flash SYBR qPCR kit (catalog no. F-415XL; Thermo-Fisher, Waltham, MA, USA) according to the recommended protocol. Reactions were performed on a Bio-Rad CFX384. Procedures for normalization and data handling are described in section 2.10 below, primer sequences are listed in Table S1.

2.9. Chromatin immunoprecipitation (ChIP) analysis

We performed chromatin Immunoprecipitations (ChIP) using a previously described protocol [15,16], with the following modifications. Briefly, 50 mg of liver tissue were thawed on ice in cold PBS and dispersed into single cell suspensions using a 100 μm cell strainer (catalog no. 352360; Corning Life Sciences, Corning, NY, USA). Cells were washed twice with PBS containing protease inhibitor cocktail (catalog no. 78437; Thermo-Fisher, Waltham, MA, USA) and resuspended in cell culture medium (DMEM F-12 catalog no. 11320-033; Thermo-Fisher, Waltham, MA, USA) containing 0.1 volume of 10x crosslinking solution (10.8% Formaldehyde, 1 M NaCl, 10 mM EDTA, 500 mM HEPES pH 7) for fifteen minutes. After quenching with 125 mM glycine for five minutes, cells were washed three times in ice-cold PBS containing protease inhibitor cocktail and lysed in ChIP lysis buffer (150 mM NaCl, 25 mM Tris·Cl, pH 7.5, 5 mM EDTA, 1% Triton X-100, 0.1% SDS, 0.5% sodium deoxycholate). Cellular extracts were sonicated with a Bioruptor sonication system (Diagenode, Denville, NJ, USA) using TPX microtubes (catalog no. C30010010; Diagenode, Denville, NJ, USA) and DNA fragment lengths visualized using agarose gel electrophoresis. Immunoprecipitations were performed with antibodies recognizing anti-LXRα (catalog no. ab41902; RRID:AB_776094; Abcam, Cambridge, MA, USA) overnight, at 4 °C, in dilution buffer (0.1% SDS, 1% Triton X-100, 2 mM EDTA, 20 mM Tris, pH 8.1, 500 mM NaCl), under constant rotation. Antibodies recognizing

rabbit IgG (catalog no. SC-2027; RRID:AB_737197; Santa Cruz, Santa Cruz, CA, USA) served as the nonspecific control. All antibodies were used at a concentration of 1 μg/ChIP reaction. Chromatin was precipitated using protein A/G sephadex beads (catalog no. 17513801 and 17061801; GE Healthcare, Marlborough, MA, USA), washed in ice-cold Low Salt Wash Buffer (0.1% SDS, 1% Triton X-100, 2 mM EDTA, 20 mM Tris, pH 8.1, 150 mM NaCl), High Salt Wash Buffer (0.1% SDS, 1% Triton X-100, 2 mM EDTA, 20 mM Tris, pH 8.1, 500 mM NaCl), LiCl Wash Buffer (0.25 M LiCl, 1% IGEPAL, 1% Deoxycholate Na, 1 mM EDTA, 10 mM Tris, pH 8.1) and eluted in 70 °C Elution Buffer (10% SDS, 1 M $NaHCO_3$). After reversing crosslinks and proteinase K digestion, DNA was isolated using a Qiaquick PCR Cleanup kit (catalog no. 28106; Qiagen, Germantown, MD, USA). For analysis of candidate loci, real-time PCR was performed using the Dynamo Flash SYBR qPCR kit (catalog no. F-415XL; Thermo-Fisher, Waltham, MA, USA) according to the recommended protocol. Reactions were performed on a Bio-Rad CFX384 Touch PCR system. Data were analyzed using the formula previously described [17]. Primer sequences of the examined loci are listed in Table S1.

2.10. Data handling, experimental replicates and statistical analysis

For all experiments, measures were input into the statistical analysis program GraphPad (RRID:SCR_002798; GraphPad Software, Inc., La Jolla, CA, USA) and statistical significance set at alpha = 0.05. All datasets were first verified for normality using the Brown-Forsythe test. In this study, the effect of two independent variables (preconception treatment versus dietary treatment) were assessed using a two-way analysis of variance test (ANOVA), and differences among the means evaluated using Sidak's post-hoc test of contrast. For

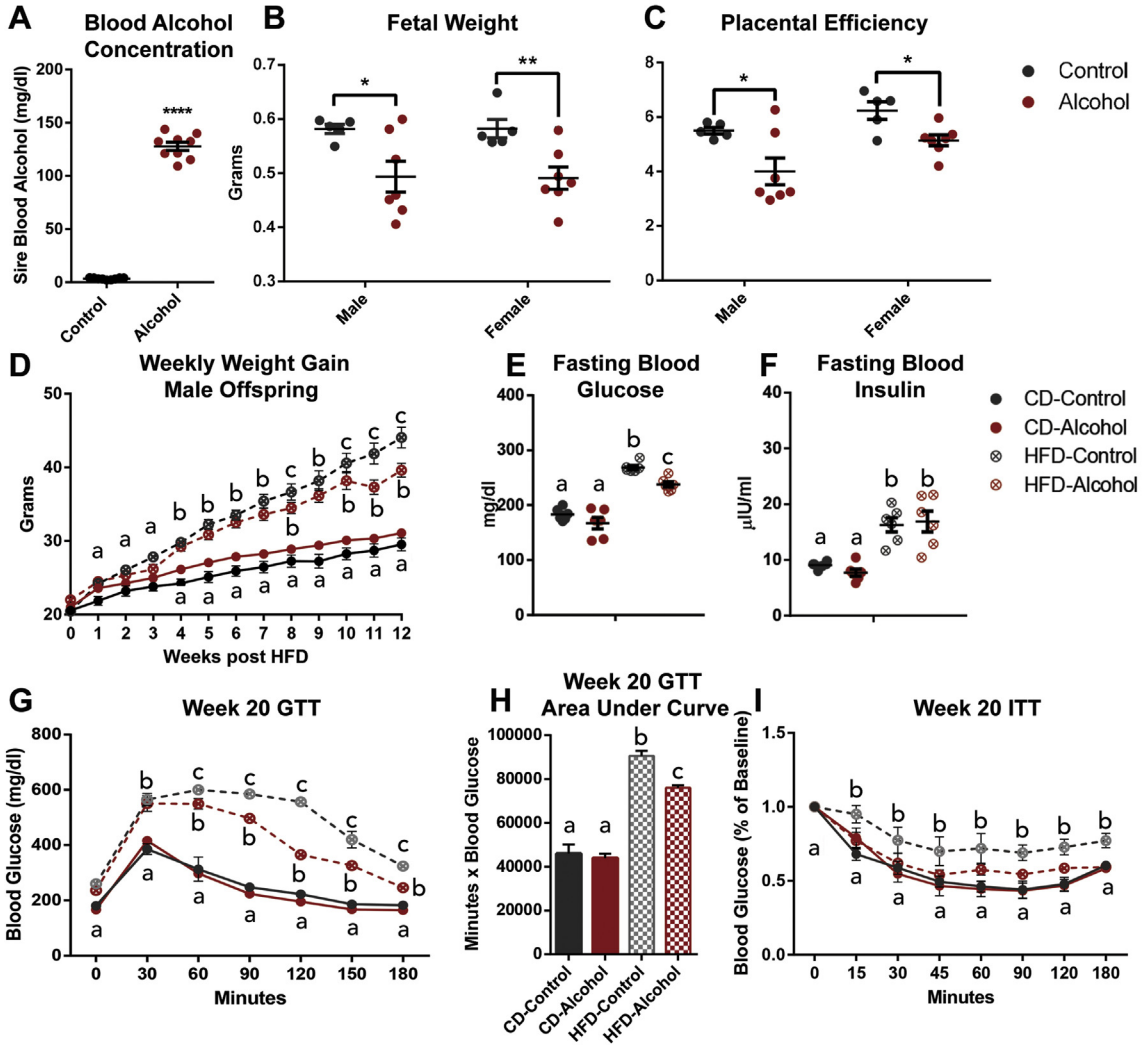

Figure 1: The male offspring of alcohol-exposed fathers display enhanced metabolic adaptation and resistance to high-fat diet-induced obesity. (A) Average blood alcohol concentrations between control and alcohol-exposed sires (n = 9, comparisons made using an unpaired t-test). (B) Comparisons of average litter weights, separated by sex, between the offspring of control and alcohol-exposed males (n = 5 litters sired by control males and 7 litters sired by alcohol-exposed males, differences assessed using a two-way ANOVA). (C) Placental efficiency (gram of fetus produced per gram of placenta) compared between litters sired by control and ethanol-exposed sires. (D) Weekly weight gain, (E) fasting blood glucose and (F) fasting insulin levels compared between the male offspring of control and alcohol-exposed fathers. (G) Glucose tolerance test (H), area under the curve analysis and (I) insulin tolerance tests comparing glucose homeostasis between the male offspring of control and alcohol-exposed fathers. Comparisons of offspring metabolism were conducted using a two-way ANOVA. Data points with distinct letter superscripts are different at $p < 0.05$. Error bars represent the SEM, *$P < 0.05$, **$P < 0.01$, and ****$P < 0.0001$.

comparisons between two treatment groups, an unpaired t-test was employed. In all instances, we have marked statistically significant differences ($p < 0.05$) with either distinct letter superscripts or an asterisk.

For the analysis of blood alcohol levels, 9 control and 9 alcohol-exposed males were compared using an unpaired t-test. For comparisons of fetal weight, we first separately averaged the weights of the male and female fetuses in each litter and then compared each group using a two-way ANOVA (n = 5 control and 7 alcohol). Placental efficiency was calculated by dividing the average fetal weight per litter by the average placental weight per litter. Male and female efficiencies were calculated separately. For the analysis of weekly weight gain for the male offspring, comparisons were made using a multi-measure two-way ANOVA (chow diet-control n = 12 males from 5 separate litters, chow diet-alcohol n = 21 males from 7 separate litters, high-fat diet-control n = 12 males from 5 separate litters, and high-fat diet-alcohol n = 21 males from 7 separate litters). For the analysis of fasting blood glucose levels, fasting blood insulin levels, and both the glucose and insulin tolerance tests, differences were compared using a two-way ANOVA (n = 6). For analyses using western blotting of LXRα, ELISA, and ChIP, as well as investigations of hepatic cholesterol levels, hepatic triglyceride levels and hepatic hydroxyproline content, values were compared using a two-way ANOVA (n = 8). For RT-qPCR analysis of gene expression, the replicate cycle threshold (Ct) values for each transcript were compiled and normalized to the geometric mean of three validated reference genes. In the liver, transcripts encoding tyrosine 3-monooxygenase/tryptophan 5-monooxygenase activation protein zeta (*Ywhaz* - NM_011740), *mitochondrial ribosomal protein L1* (*Mrpl1* - NM_053158) and *hypoxanthine-phosphoribosyl transferase* (*Hprt*—NM_013556) were measured as reference genes. In the pancreas and visceral fat, transcripts encoding *H2A Histone Family Member Z* (*H2afz* - NM_001316995), *mitochondrial ribosomal protein L1* (*Mrpl1* - NM_053158) and *hypoxanthine-phosphoribosyl transferase* (*Hprt*—NM_013556) served as reference genes. Each of these reference genes were validated for stability across treatment groups using methods described previously [18]. Normalized expression levels

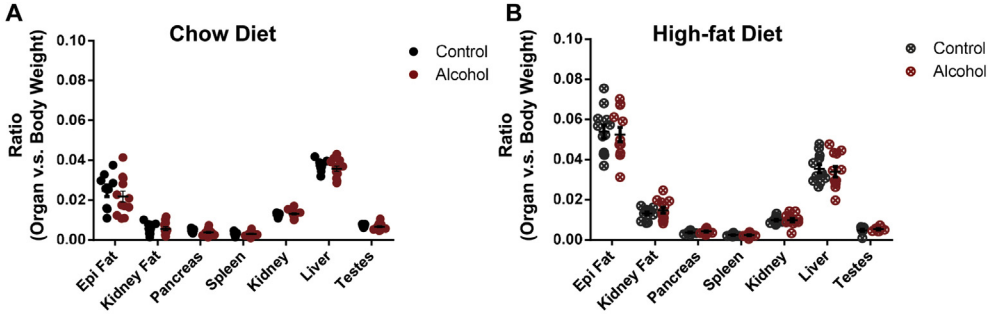

Figure 2: Preconception paternal alcohol exposure does not alter organ weights in the adult offspring. Organ weights of the male offspring of control and alcohol-exposed sires in the **A)** CD and **B)** HFD postnatal treatment groups. Using a two-way ANOVA, differences in epididymal and kidney fat deposits were identified between the two dietary treatments. No other organs were significantly different. No differences ($p < 0.05$) were identified between the preconception treatment groups (CD Control n = 9, CD Alcohol n = 12, HFD Control n = 12, HFD Alcohol n = 12).

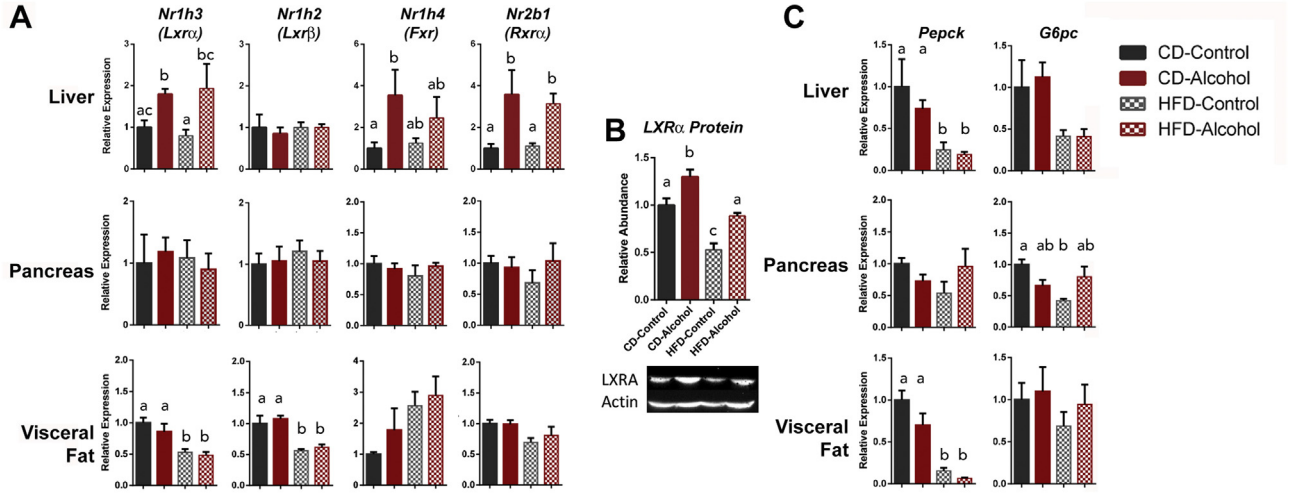

Figure 3: Liver-specific, programed upregulation of Liver X Receptor alpha in the male offspring of alcohol-exposed fathers. (A) RT-qPCR analysis of nuclear receptor expression in the liver, pancreas and visceral fat. (B) Western blot analysis of hepatic LXRα expression. (C) RT-qPCR analysis of LXRα-regulated glycogenic genes in the liver, pancreas and visceral fat. Statistical comparisons made using a two-way ANOVA contrasting dietary and preconception treatments (n = 8). For RT-qPCR analysis of gene expression, the replicate cycle threshold (Ct) values for each transcript were compiled and normalized to the geometric mean of three validated reference genes (see section 2.10). Error bars represent the SEM, data points with distinct letter superscripts are different at $p < 0.05$.

were calculated using the ddCt method described previously [19]. Relative fold change values from each biological replicate were determined using Microsoft Excel, values transferred into the statistical analysis program GraphPad and differences assessed using a two-way ANOVA (n = 8).

3. RESULTS

3.1. Preconception paternal alcohol exposure protects offspring from diet-induced obesity and improves metabolic adaptation

Previously, in the offspring of alcohol-exposed males, we identified increased stimulation of genetic pathways regulated by Liver X receptors [7]. As the male offspring of alcohol-exposed sires demonstrated deficits in both growth and metabolic health, which persisted into adolescence, we focused our analyses exclusively on this sex. Similar to multigenerational studies examining the offspring of IUGR males [9], RNA-sequencing analysis of the adolescent liver could not identify any differential expression of known *Lxr* transcriptional regulators, including PPARα, PPARϒ, and HNF4A (Table S2). To determine if programmed increases in LXR activity could improve metabolic adaptation and protect the male offspring of alcohol-exposed sires from diet-induced obesity, we returned to our model of chronic paternal alcohol consumption and exposed postnatal day 90 adult males to either the preconception control or alcohol treatments. We did not observe any differences in weight gain or fluid consumption between the two preconception treatment groups (Figs. S1A–C). Plasma alcohol levels averaged 127 mg/dL, and, similar to previous studies, matings between alcohol-exposed sires and naive females produced growth-restricted offspring, as measured at gestational day 16.5 (Figure 1A–B). This growth restriction was accompanied by a significant reduction in placental efficiency (Figure 1C).

To determine the postnatal response of alcohol-exposed offspring to a high-fat dietary challenge, we randomly assigned male littermates sired by alcohol-exposed and control fathers between standard chow (CD) and high-fat diet (HFD) treatment groups. We did not observe any differences in food consumption between the alcohol or control preconception treatment groups for either dietary treatment (Fig. S1D). After 3 weeks of exposure to a HFD, male offspring from both preconception treatment groups were significantly heavier than animals maintained on the CD (Figure 1D, p-value = 0.0013). However, after 8-weeks HFD treatment, male offspring sired by alcohol-exposed fathers displayed significant reductions in weekly weight gain as compared to the male offspring of control fathers (Figure 1D, $p < 0.001$ weeks 11 & 12). In the male offspring of alcohol-exposed sires maintained on a HFD, we observed a ~10% reduction in fasting blood glucose levels, while fasting insulin concentrations were identical between the two preconception treatment groups (Figure 1E–F). In the HFD treatment group, the observed reductions in blood glucose concentrations and weekly weight gain observed in the offspring of alcohol-exposed sires also associated with improved performance in both glucose and insulin tolerance tests, as compared to offspring sired by control males (Figure 1G–I, Fig. S2). Collectively, these observations indicate that the male offspring of alcohol-exposed sires exhibit modest protection from high-fat diet-induced obesity and improved glucose homeostasis under conditions associated with obesity-induced insulin resistance.

3.2. Liver-specific alterations in LXRα programming associate with suppression of proinflammatory NFkB target genes

After 12-weeks of treatment (20 weeks postnatal life), mice were terminated and tissues collected. Although we detected an increase in both epididymal and kidney fat in the HFD treatment group, we did not observe any other differences in organ weights between dietary treatments. More importantly, preconception treatment did not influence organ weight (Figure 2A–B). Using RT-qPCR, we examined the expression of liver x receptors alpha and beta as well as known binding partners, including the farnesoid x and retinoid x alpha receptors, in the liver (gene names *Nr1h3*, *Nr1h2*, *Nr1h4*, and *Nr2b1*, respectively). The

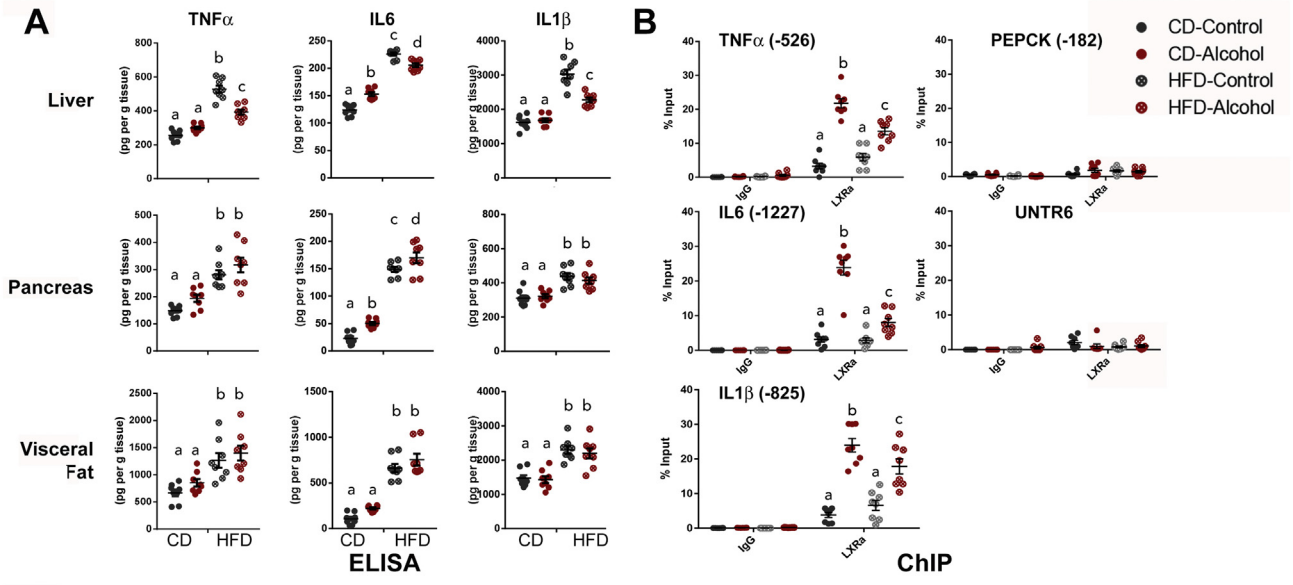

Figure 4: Programed increases in Liver X Receptor alpha suppresses NFκB inflammatory cytokine production in the male offspring of alcohol-exposed fathers. (A) ELISA analysis contrasting the abundance of inflammatory cytokines in the liver, pancreas and visceral fat. (B) Chromatin immunoprecipitation analysis of LXRα enrichment on the regulatory regions of the indicated genes within the liver. Comparisons made between the male offspring of control and alcohol-exposed sires, within and across the two dietary treatments, using a two-way ANOVA (n = 8). Error bars represent the SEM, data points with distinct letter superscripts are different at $p < 0.05$.

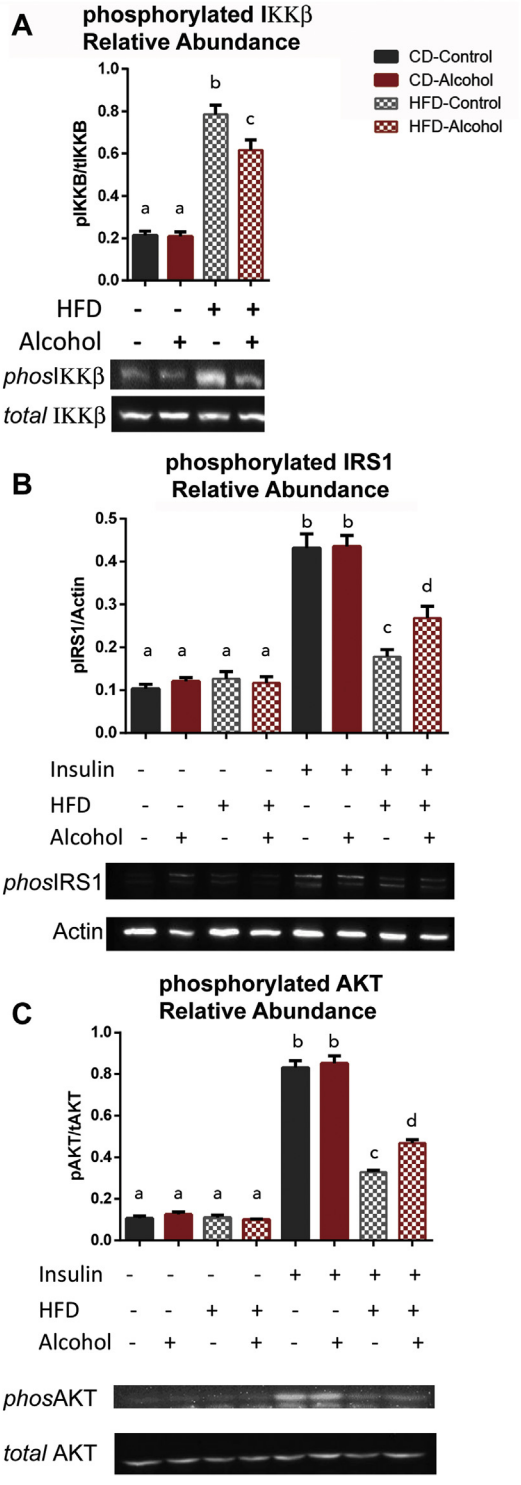

Figure 5: Reduced Ikkβ inhibition and enhanced hepatic insulin signaling in the male offspring of alcohol-exposed fathers. Relative abundance of phosphorylated (A) Ikkβ, (B) IRS1 and (C) AKT were compared between the livers of the male offspring of control and alcohol-exposed sires (CD=Chow Diet, HFD=High-Fat Diet). Comparisons made using a two-way ANOVA contrasting dietary and preconception treatments ($n = 6$). Error bars represent the SEM. Data points with distinct letter superscripts are different at $p < 0.05$.

expression of *Lxrα* and *Rxrα* were significantly increased in the male offspring of alcohol-exposed fathers, regardless of dietary treatment (Figure 3A). Although we did observe increased *Fxr* transcript levels, it was only in mice maintained on the standard chow diet and not under the HFD treatment. We did not observe any differences in *Lxrβ* transcripts in any treatment group. Increased expression of *Lxrα* in the male offspring of alcohol-exposed sires was confirmed using western blotting (Figure 3B). In contrast to what we observed in the liver, we did not observe any preconception treatment-associated changes in gene expression within other metabolically relevant tissues, including the pancreas and visceral fat (Figure 3A).

In the liver, LXRα is known to suppress glycogenic pathways through direct binding of the promoters of genes encoding phosphoenolpyruvate carboxykinase (PEPCK) and glucose-6-phosphatase catalytic subunit (G6PC) [11,13]. Suppression of these genes could explain some of the improvements in glucose homeostasis observed in the male offspring of alcohol-exposed fathers maintained on a high-fat diet. However, we could not detect any preconception treatment-associated differences in the expression of either gene in any tissue (Figure 3C).

In addition to regulating both cholesterol and glucose homeostasis, LXRα also exerts anti-inflammatory effects by repressing the production of a core set of nuclear factor k B (NFkB)-induced inflammatory cytokines [20–22]. Through interactions with Toll-like receptors (TLRs) and the inhibitor of nuclear factor k B Kinase β (Ikkβ) complex, NFkB inflammatory cytokines are powerful suppressors of insulin signaling [23,24]. We hypothesized that the alleviation of this inhibitory influence by increased LXRα activity could be responsible for the improved glucose homeostasis observed in our model. Therefore, we compared the abundance of a core group of metabolically relevant inflammatory cytokines between the male offspring of alcohol-exposed and control fathers, across both dietary treatment groups (Figure 4A). As expected, we observed increased cytokine abundance in the tissues of males maintained on the HFD treatment when compared to the chow-fed mice. However, in the livers of the male offspring of alcohol-exposed sires maintained on a HFD, we observed significant reductions in the levels of TNFα, IL1β, and IL6, as compared to the HFD-fed offspring of control males. These reductions were specific to the liver and did not appear in either the pancreas or visceral fat. Similar to our previous studies [7], we could not detect TNFα, IL1β, or IL6 in circulation. With the exception of IL6 in the pancreas, we did not observe any differences in cytokine abundance in animals maintained on the standard chow diet.

When SUMOylated, agonist-bound LXRα exerts trans-repressive activity by forming a complex with the N-CoR (*nuclear receptor corepressor*) and/or SMRT (*silencing mediator for retinoid and thyroid hormone receptors*) corepressor complexes on NFκB target genes [22,25,26]. Using chromatin immunoprecipitation, we assayed the enrichment of LXRα at known *p50* binding sites within the promoter regions of TNFα, IL1β, and IL6, as well as in the previously identified LXRα binding site in the promoter region of the *Pepck* gene [13,27]. In these experiments, enrichment of LXRα at an untranscribed region of chromosome 6 (Untr6) served as a non-specific control [28]. In both dietary treatment groups, the male offspring of alcohol-exposed fathers exhibited a 10–20% increase in the enrichment of LXRα on the TNFα, IL1β, and IL6 gene promoters (Figure 4B). Enrichment of LXRα was modestly higher in males maintained on the chow diet as compared to those in the HFD treatment group ($p < 0.05$). Unlike the proinflammatory NFκB target genes examined, the promoter region of *Pepck* did not exhibit any LXRα enrichment and remained equivalent to

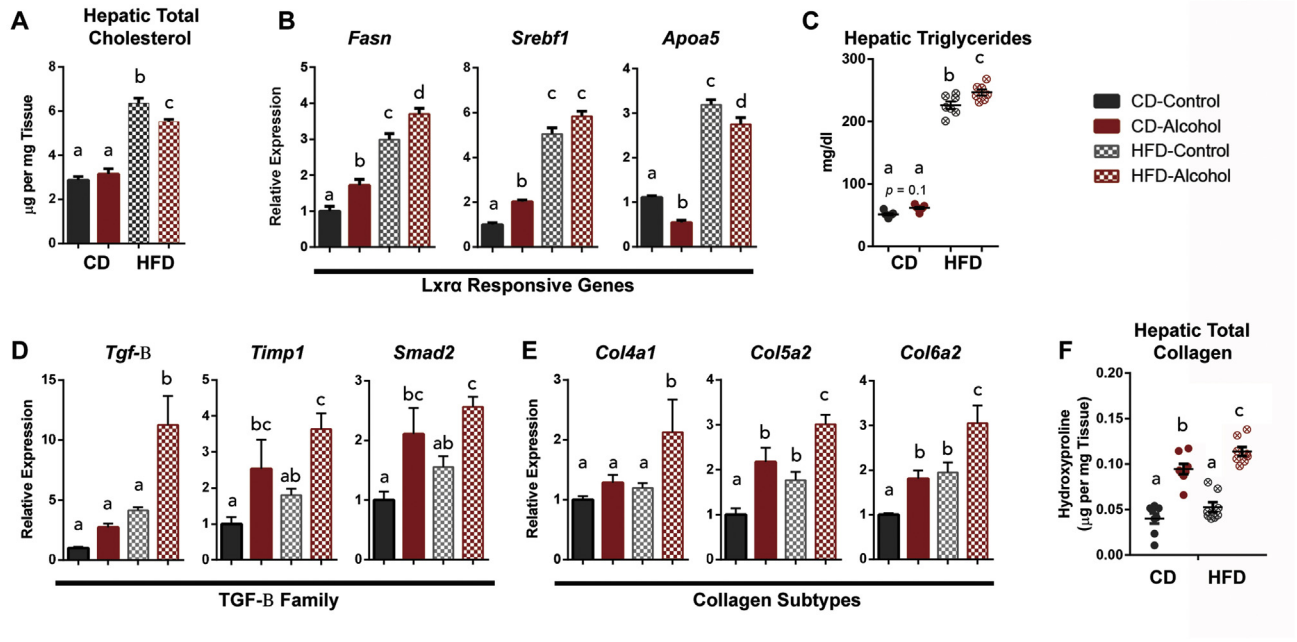

Figure 6: Programed increases in LXRα expression induce hypertriglyceridemia, which correlates with increased hepatic fibrosis in the male offspring of alcohol-exposed fathers. Analyses contrasting hepatic tissues from the male offspring of control and alcohol-exposed sires, across and within the two dietary treatments. (A) Hepatic cholesterol levels, (B) RT-qPCR analysis of LRXα-regulated lipogenic genes, (C) hepatic triglyceride levels, RT-qPCR analysis of genes encoding pro-fibrotic (D) signaling and (E) structural proteins, and (F) total levels of cellular hydroxyproline. Comparisons made using a two-way ANOVA (n = 8). Error bars represent SEM, data points with distinct letter superscripts are different at $p < 0.05$.

the non-specific control. Collectively, these observations indicate that the offspring of alcohol-exposed sires exhibit liver-specific programmed enhancement of LXRα but not LXRβ, which associates with increased binding at NFκB target genes and reductions in the production of inflammatory cytokines.

3.3. Enhanced insulin signaling in the offspring of alcohol-exposed sires

Mice carrying a hepatocyte-specific genetic deletion of toll-like receptor 4 (TLR4) exhibit enhanced insulin sensitivity, similar in magnitude to that observed in our model [29]. To explore the impact LXRα-mediated reductions in cytokine production have on insulin signaling, we began by assaying the phosphorylation status of Ikkβ. Ikkβ is directly downstream of TLR4 and becomes phosphorylated upon cytokine stimulation. Using western blot analysis, we identified a ~20% reduction in phosphorylated (Tyr 199) I*kkβ* in the male offspring of alcohol-exposed sires maintained on the HFD but not in males maintained on the chow diet (Figure 5A). The inhibitory effects of I*kkβ* on insulin signaling are primarily mediated by blocking the association of insulin receptor substrate 1 (IRS1) with the p85 subunit of phosphatidylinositol 3-kinase [23,24]. Therefore, we quantified levels of phosphorylated IRS1 in insulin perfused livers of the offspring of alcohol-exposed and control males under both dietary treatments. We observed a ~50% increase in phosphorylated (Ser 307) IRS1 in the insulin perfused litters of the male offspring of alcohol-exposed sires maintained on a HFD, while male offspring maintained on the chow diet did not exhibit any identifiable changes (Figure 5B). Consistent with increased levels of phosphorylated IRS1, we observed a corresponding ~45% increase in phosphorylated (Ser 473) Akt in the male offspring of alcohol-exposed sires maintained on a HFD (Figure 5C). These observations indicate that, in the male offspring of alcohol-exposed sires, LXRα mediated decreases in cytokine production alleviate Ikkβ-mediated inhibition of insulin signaling, which enhances metabolic adaptation to a high-fat diet.

3.4. LXRα-induced alterations in lipid metabolism and increased hepatic fibrosis in the offspring of alcohol-exposed sires

Given that paternally-inherited increases in LXRα activity were able to moderate the effects of a high-fat diet, we next examined other metabolic outcomes associated with the use of LXR agonists. In previous studies, treatment with LXR agonists decreased levels of hepatic cholesterol by engaging the genetic pathways driving cholesterol efflux [30]. Similar to mice treated with the non-steroidal LXRα-specific agonist T0901317 [31,32], we observed a ~15% decrease in total hepatic cholesterol levels in the male offspring of alcohol-exposed sires maintained on a HFD (Figure 6A). No differences in the proportion of either LDLs or HDLs were observed (Figs. S3A–C). In contrast, we did not observe any differences in total cholesterol levels in male offspring maintained on the standard chow diet. Although synthetic LXR agonists inhibit atherosclerosis, their efficacy as therapeutic agents is complicated by the fact that they cause hepatic steatosis and hypertriglyceridemia [31]. Hepatic steatosis is postulated to be the consequence of increased fatty acid synthesis caused by the induction of lipogenic enzymes, including fatty acid synthase (FASN) and sterol regulatory element binding transcription factor 1 (SREBF1). Consistent with studies examining LXR agonists [31], we observed a ~15–20% induction of *Fasn* in the male offspring of alcohol-exposed sires across both dietary treatments. Although levels of *Srebf1* appeared to follow a similar trend, transcript levels were only significantly increased in animals maintained on the chow diet and not under the HFD treatment ($p < 0.05$, Figure 6B). However, in previous studies, agonist-induced activation of LXR signaling led to Srebf1-mediated suppression of *Apolipoprotein A5* [33]. Similar to this report, we observed a significant decrease in *Apoa5* transcript levels in the offspring of alcohol-exposed

sires across both dietary treatments (Figure 5B). Finally, consistent with the increased expression of lipogenic enzymes, we observed a ~10% increase in hepatic triglyceride levels in the male offspring of alcohol-exposed sires maintained on a HFD, indicating the emergence of steatosis in the offspring of alcohol-exposed sires (Figure 6C).

Hepatic steatosis is considered part of the spectrum of nonalcoholic fatty liver diseases and has been linked to the emergence of hepatic fibrosis [34]. In our previous studies, the male offspring of alcohol-exposed sires displayed transcriptional up-regulation of TGF-β-driven pathways and increased expression of multiple collagen subtypes, which associated with increased markers of fibrosis at 8-weeks postnatal life [7]. To determine the impact treatment with a HFD had on the expression of TGF-β-driven profibrotic genes, we assayed the expression of the previously identified candidate genes using RT-qPCR. In the male offspring of alcohol-exposed sires maintained on an HFD, we observed an increased abundance of transcripts encoding *Tgf-β*, *Timp1*, and *Smad2*, as well as the collagen subtypes *Col4a1*, *Col5a2*, and *Col6a2* (Figure 6D–E). We correlated this transcriptional up-regulation with a 50% increase in levels of liver hydroxyproline (Figure 6F), an established marker of hepatic fibrosis [35]. Importantly, this signature of fibrosis was present in the offspring of alcohol-exposed sires regardless of dietary treatment but became exacerbated under the HFD treatment.

3.5. Up-regulation of LXRα is not observed during development of the fetal liver

Having identified a plausible molecular explanation to the enhanced insulin sensitivity, we next focused on determining when during the life-course of the offspring LXRα expression became up-regulated. In previous studies, we identified increased LXRα activity at 8-weeks of age [7]. However, when this up-regulation first appears is not known. To this end, we returned to the fetal tissues collected in section 3.1 and using RT-qPCR, assayed expression patterns in the fetal liver at gestational day 16.5. We did not identify any differences in expression for LXRα or any of the other nuclear receptors examined in this study (Figure 7). From these data, we conclude that the up-regulation of LXRα occurs postnatally and does not drive the observed fetal growth restriction.

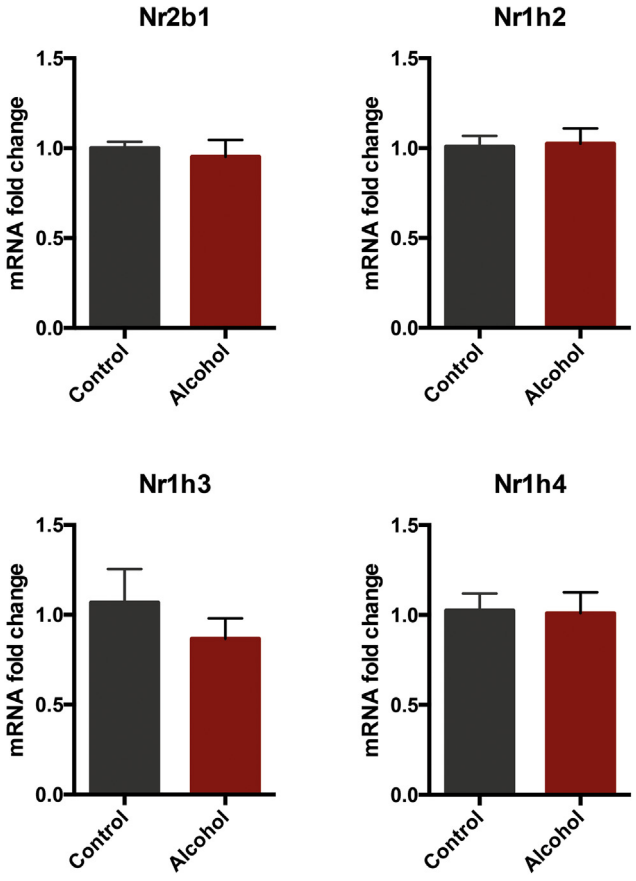

Figure 7: Up-regulation of LXRα is not observed during development of the fetal liver. RT-qPCR analysis of the indicated nuclear receptors in the gestational day 16.5 fetal liver. Comparisons made between the male offspring of control and alcohol-exposed sires. No differences were noted between preconception treatment groups ($p < 0.05$).

4. DISCUSSION

Liver X receptors function as dynamic regulators of cholesterol metabolism and lipid biosynthesis but also sensitize the insulin signaling pathway and suppress the innate immune system [10]. Despite these far reaching effects, the contribution of this nuclear receptor family to the metabolic phenotypes observed in models of altered developmental programming remain poorly described. Consistent with studies examining the effects of Liver X Receptor agonists [11,31], the male offspring of alcohol-exposed sires displayed enhanced metabolic adaptation and slowed weight gain when challenged with a high-fat diet, as well as several of the undesirable side effects of LXR stimulation, including increased hepatic cholesterol efflux and hypertriglyceridemia. Based on our experimental data, we propose that liver-specific increases in LXRα suppress NFkB driven production of inflammatory cytokines, which relieves I*k*kβ-mediated repression of the insulin signaling pathway, and leads to the increased insulin sensitivity observed in the male offspring of alcohol-exposed males (Figure 8).

Unexpectedly, we only observed differences in glucose homeostasis and insulin signaling following the HFD treatment, while in our previous studies, we readily observed these phenotypes in the male offspring maintained on a CD [7]. We propose that these disparities are due to differences in the age of the offspring between the two experiments. Our previous work focused on 8-week-old offspring, while, in contrast, this study focused on 20-week-old offspring. While some aspects of the molecular phenotype we described in 8-week-old males were consistent, for example, increased TGF-β signaling and hepatic collagen levels, the metabolic phenotypes only manifested in offspring experiencing the stress of a high-fat diet. We suspect that as the male offspring of alcohol-exposed sires age, their physiology normalizes, and both insulin signaling and glucose homeostasis move closer to the controls. However, consistent with other models of altered programming, the underlying epigenetic changes persist, and programmed differences in gene regulation reemerge upon exposure of the offspring to a stressor.

Another seemingly contradictory finding to come out of this study is the observation that whole body glucose homeostasis improved despite indicators of increased triglyceride production and hepatic steatosis. Indeed, although liver steatosis is generally associated with insulin resistance and reduced glucose tolerance [36], we observed an increase in insulin sensitivity in male offspring of alcohol-treated fathers. One potential explanation for this is that the increased free fatty acids produced by the liver remain stored in this organ are not released into circulation. As a consequence, the systemic effects of HFD-induced

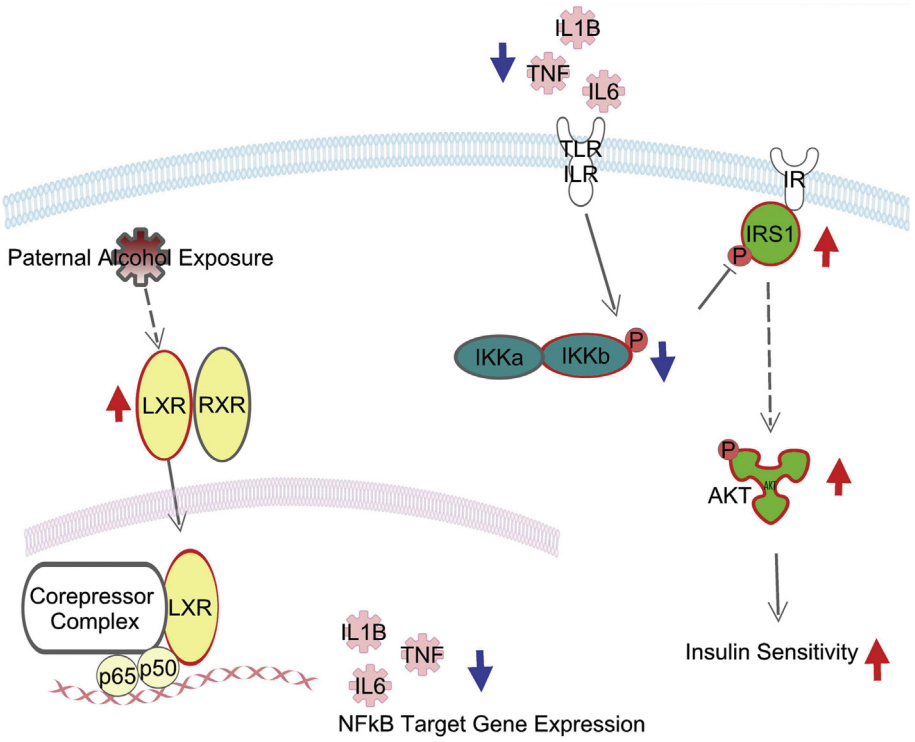

Figure 8: Proposed model. Programmed increases in hepatic LXRα suppress production of inflammatory cytokines, which relieves Ikkβ-mediated inhibition of the insulin signaling pathway and increases insulin sensitivity in the male offspring of alcohol-exposed sires.

lipotoxicity decrease due to the lack of TLR-inhibition of insulin signaling. However, our experiments did not measure insulin sensitivity in either muscle or adipocytes, and therefore, we cannot exclude the involvement of mechanisms other than those mediated by LXRα.

Despite characterizing the basis to the altered insulin signaling in the liver, the molecular mechanisms by which the memory of paternal alcohol exposures persists into the next generation and influence LXRα activity remain unknown. Our previous studies identified sex-specific alterations in TGF-β signaling, which were first observed in the fetal liver and persisted to 8-weeks postnatal life [5,7]. In mice, TGF-β stimulation induces hepatic lipogenesis and treatment with a HFD is known to exacerbate the stimulation of these pathways [37]. It is possible that in the male offspring of alcohol-exposed sires, LXRα is induced to compensate for the TGF-β-mediated increases in lipids by converting them to triglycerides and, as a consequence, also suppresses the production of inflammatory cytokines and improves hepatic insulin signaling under a HFD treatment. Recently, phosphorylation of LXRα-serine 196 was identified as a major component of the pathways driving hepatic fibrosis during the development of non-alcoholic fatty liver disease [38,39]. Our experimental data may indicate that TGF-β-driven fibrosis can, in turn, induce LXRα activity. However, additional experiments are necessary to confirm this reciprocal relationship.

Multiple studies have suggested that changes in sperm DNA methylation persist through early development and exert a lasting influence on offspring physiology, while others indicate a causative role for sperm-inherited noncoding RNAs [40]. However, despite the fact that multiple models of compromised paternal programming consistently exert long-term effects on offspring metabolism, the majority of which appear to converge on the regulation of glucose and lipid homeostasis, no consistent cohort of differentially methylated loci or population of small RNA has been identified that can explain the observed changes in metabolic function. Although Martinez et al., identified reductions in DNA methylation within the *Lxrα* 5′ UTR that were consistent between sperm and the resulting offspring [9], we were unable to identify any changes in DNA methylation within the sperm of alcohol-exposed males [5]. However, the 2% change identified by Martínez et al., was below our threshold of detection. Further, although we and others have described alcohol-induced changes in sperm-inherited noncoding RNAs [6,41], the identified candidates have either been inconsistent with other metabolically focused studies or associated with deficits in glucose homeostasis and increased susceptibility to the effects of a high-fat diet. Interestingly, none of the nuclear receptors examined in this study were differentially expressed in the fetal liver (Figure 7), indicating that the up-regulation of LXRα activity in the adult offspring of alcohol-exposed sires is very likely a downstream outcome of altered paternal programming rather than the direct epigenetic memory. The identification of compromised placentation in this and other models of paternal programming suggest the strong possibility that the sex- and tissue-specific effects observed are all secondary symptoms of a compromised maternal-fetal interface [42].

4.1. CONCLUSIONS

The life expectancy of patients with fetal alcohol syndrome is 34 years, which is 58% lower than that of the general population [43]. Although clinical studies can correlate maternal alcohol exposures during gestation with dose- and sex-dependent effects on the metabolic health of the offspring [44,45], no studies to date have examined the long-term consequences of paternal alcohol use on offspring growth

and metabolic health. If the phenomenon we observe in our mouse model translates to humans, our findings indicate that paternal alcohol use may well be a relevant factor to the immune and metabolic disturbances observed in FASDs and that LXR signaling pathways are key mediators of these effects. Researchers in the field must now extend their perspective beyond maternal models of exposure and more carefully consider the importance of paternal lifestyle to the developmental origins of alcohol-induced disease.

AUTHOR CONTRIBUTIONS

R.C.C. and M.C.G. designed the experiments and analyzed the data; R.C.C., Y.S.B., and K.N.T. performed the research; M.C.G. wrote the paper.

ACKNOWLEDGMENTS

The authors gratefully acknowledge the technical assistance of researchers within the TIGM transgenic mouse core. This work was supported by a research grant from the W.M. Keck foundation.

CONFLICT OF INTEREST

The authors declare that they have no competing interests.

APPENDIX A. SUPPLEMENTARY DATA

Supplementary data to this article can be found online at https://doi.org/10.1016/j.molmet.2019.09.016.

REFERENCES

[1] Lane, M., Robker, R.L., Robertson, S.A., 2014. Parenting from before conception. Science 345:756–760.

[2] Fleming, T.P., Watkins, A.J., Velazquez, M.A., Mathers, J.C., Prentice, A.M., Stephenson, J., et al., 2018. Origins of lifetime health around the time of conception: causes and consequences. Lancet 391:1842–1852.

[3] Rompala, G.R., Homanics, G.E., 2019. Intergenerational effects of alcohol: a review of paternal preconception ethanol exposure studies and epigenetic mechanisms in the male germline. Alcoholism: Clinical and Experimental Research 43:1032–1045.

[4] Finegersh, A., Rompala, G.R., Martin, D.I., Homanics, G.E., 2015. Drinking beyond a lifetime: new and emerging insights into paternal alcohol exposure on subsequent generations. Alcohol 49:461–470.

[5] Chang, R.C., Skiles, W.M., Chronister, S.S., Wang, H., Sutton, G.I., Bedi, Y.S., et al., 2017. DNA methylation-independent growth restriction and altered developmental programming in a mouse model of preconception male alcohol exposure. Epigenetics 12:841–853.

[6] Bedi, Y., Chang, R.C., Gibbs, R., Clement, T.M., Golding, M.C., 2019. Alterations in sperm-inherited noncoding RNAs associate with late-term fetal growth restriction induced by preconception paternal alcohol use. Reproductive Toxicology 87:11–20.

[7] Chang, R.C., Wang, H., Bedi, Y., Golding, M.C., 2019. Preconception paternal alcohol exposure exerts sex-specific effects on offspring growth and long-term metabolic programming. Epigenetics & Chromatin 12:9.

[8] Rompala, G.R., Finegersh, A., Slater, M., Homanics, G.E., 2017. Paternal preconception alcohol exposure imparts intergenerational alcohol-related behaviors to male offspring on a pure C57BL/6J background. Alcohol 60:169–177.

[9] Martínez, D., Pentinat, T., Ribó, S., Daviaud, C., Bloks, V., Cebrià, J., et al., 2014. In utero undernutrition in male mice programs liver lipid metabolism in the second-generation offspring involving altered lxra DNA methylation. Cell Metabolism 19:941–951.

[10] Maqdasy, S., Trousson, A., Tauveron, I., Volle, D.H., Baron, S., Lobaccaro, J.M., 2016. Once and for all, LXRα and LXRβ are gatekeepers of the endocrine system. Molecular Aspects of Medicine 49:31–46.

[11] Laffitte, B.A., Chao, L.C., Li, J., Walczak, R., Hummasti, S., Joseph, S.B., et al., 2003. Activation of liver X receptor improves glucose tolerance through coordinate regulation of glucose metabolism in liver and adipose tissue. Proceedings of the National Academy of Sciences of the United States of America 100:5419–5424.

[12] Commerford, S.R., Vargas, L., Dorfman, S.E., Mitro, N., Rocheford, E.C., Mak, P.A., et al., 2007. Dissection of the insulin-sensitizing effect of liver X receptor ligands. Molecular Endocrinology 21:3002–3012.

[13] Herzog, B., Hallberg, M., Seth, A., Woods, A., White, R., Parker, M.G., 2007. The nuclear receptor cofactor, receptor-interacting protein 140, is required for the regulation of hepatic lipid and glucose metabolism by liver X receptor. Molecular Endocrinology 21:2687–2697.

[14] Overmyer, K.A., Thonusin, C., Qi, N.R., Burant, C.F., Evans, C.R., 2015. Impact of anesthesia and euthanasia on metabolomics of mammalian tissues: studies in a C57BL/6J mouse model. PLoS One 10:e0117232.

[15] Veazey, K.J., Parnell, S.E., Miranda, R.C., Golding, M.C., 2015. Dose-dependent alcohol-induced alterations in chromatin structure persist beyond the window of exposure and correlate with fetal alcohol syndrome birth defects Epigenetics and Chromatin, vol. 8. p. 1–19.

[16] Veazey, K.J., Wang, H., Bedi, Y.S., Skiles, W.M., Chang, R.C., Golding, M.C., 2017. Disconnect between alcohol-induced alterations in chromatin structure and gene transcription in a mouse embryonic stem cell model of exposure. Alcohol 60:121–133.

[17] Mukhopadhyay, A., Deplancke, B., Walhout, A.J., Tissenbaum, H.A., 2008. Chromatin immunoprecipitation (ChIP) coupled to detection by quantitative real-time PCR to study transcription factor binding to DNA in Caenorhabditis elegans. Nature Protocols 3:698–709.

[18] Carnahan, M.N., Veazey, K.J., Muller, D., Tingling, J.D., Miranda, R.C., Golding, M.C., 2013. Identification of cell-specific patterns of reference gene stability in quantitative reverse-transcriptase polymerase chain reaction studies of embryonic, placental and neural stem models of prenatal ethanol exposure. Alcohol 47:109–120.

[19] Schmittgen, T.D., Livak, K.J., 2008. Analyzing real-time PCR data by the comparative C(T) method. Nature Protocols 3:1101–1108.

[20] Joseph, S.B., Castrillo, A., Laffitte, B.A., Mangelsdorf, D.J., Tontonoz, P., 2003. Reciprocal regulation of inflammation and lipid metabolism by liver X receptors. Nature Medicine 9:213–219.

[21] Zelcer, N., Tontonoz, P., 2006. Liver X receptors as integrators of metabolic and inflammatory signaling. Journal of Clinical Investigation 116:607–614.

[22] Im, S.S., Osborne, T.F., 2011. Liver x receptors in atherosclerosis and inflammation. Circulation Research 108:996–1001.

[23] Arkan, M.C., Hevener, A.L., Greten, F.R., Maeda, S., Li, Z.W., Long, J.M., et al., 2005. IKK-beta links inflammation to obesity-induced insulin resistance. Nature Medicine 11:191–198.

[24] Cai, D., Yuan, M., Frantz, D.F., Melendez, P.A., Hansen, L., Lee, J., et al., 2005. Local and systemic insulin resistance resulting from hepatic activation of IKK-beta and NF-kappaB. Nature Medicine 11:183–190.

[25] Ghisletti, S., Huang, W., Jepsen, K., Benner, C., Hardiman, G., Rosenfeld, M.G., et al., 2009. Cooperative NCoR/SMRT interactions establish a corepressor-based strategy for integration of inflammatory and anti-inflammatory signaling pathways. Genes & Development 23:681–693.

[26] Courtney, R., Landreth, G.E., 2016. LXR regulation of brain cholesterol: from development to disease. Trends in Endocrinology and Metabolism 27:404–414.

[27] Falvo, J.V., Tsytsykova, A.V., Goldfeld, A.E., 2010. Transcriptional control of the TNF gene. Current Directions in Autoimmunity 11:27–60.

[28] Vakili, H., Jin, Y., Menticoglou, S., Cattini, P.A., 2013. CCAAT-enhancer-binding protein β (C/EBPβ) and downstream human placental growth hormone genes are targets for dysregulation in pregnancies complicated by maternal obesity. Journal of Biological Chemistry 288:22849–22861.

[29] Jia, L., Vianna, C.R., Fukuda, M., Berglund, E.D., Liu, C., Tao, C., et al., 2014. Hepatocyte Toll-like receptor 4 regulates obesity-induced inflammation and insulin resistance. Nature Communications 5:3878.

[30] Naik, S.U., Wang, X., Da Silva, J.S., Jaye, M., Macphee, C.H., Reilly, M.P., et al., 2006. Pharmacological activation of liver X receptors promotes reverse cholesterol transport in vivo. Circulation 113:90–97.

[31] Grefhorst, A., Elzinga, B.M., Voshol, P.J., Plösch, T., Kok, T., Bloks, V.W., et al., 2002. Stimulation of lipogenesis by pharmacological activation of the liver X receptor leads to production of large, triglyceride-rich very low density lipoprotein particles. Journal of Biological Chemistry 277:34182–34190.

[32] Xie, Y., Kennedy, S., Sidhu, R., Luo, J., Ory, D.S., Davidson, N.O., 2012. Liver X receptor agonist modulation of cholesterol efflux in mice with intestine-specific deletion of microsomal triglyceride transfer protein. Arteriosclerosis, Thrombosis, and Vascular Biology 32:1624–1631.

[33] Jakel, H., Nowak, M., Moitrot, E., Dehondt, H., Hum, D.W., Pennacchio, L.A., et al., 2004. The liver X receptor ligand T0901317 down-regulates APOA5 gene expression through activation of SREBP-1c. Journal of Biological Chemistry 279:45462–45469.

[34] Bataller, R., Brenner, D.A., 2005. Liver fibrosis. Journal of Clinical Investigation 115:209–218.

[35] Ding, N., Yu, R.T., Subramaniam, N., Sherman, M.H., Wilson, C., Rao, R., et al., 2013. A vitamin D receptor/SMAD genomic circuit gates hepatic fibrotic response. Cell 153:601–613.

[36] Borén, J., Taskinen, M.R., Olofsson, S.O., Levin, M., 2013. Ectopic lipid storage and insulin resistance: a harmful relationship. Journal of Internal Medicine 274:25–40.

[37] Yang, L., Roh, Y.S., Song, J., Zhang, B., Liu, C., Loomba, R., et al., 2014. Transforming growth factor beta signaling in hepatocytes participates in steatohepatitis through regulation of cell death and lipid metabolism in mice. Hepatology 59:483–495.

[38] Griffett, K., Welch, R.D., Flaveny, C.A., Kolar, G.R., Neuschwander-Tetri, B.A., Burris, T.P., 2015. The LXR inverse agonist SR9238 suppresses fibrosis in a model of non-alcoholic steatohepatitis. Molecular Metabolism 4:353–357.

[39] Becares, N., Gage, M.C., Voisin, M., Shrestha, E., Martin-Gutierrez, L., Liang, N., et al., 2019. Impaired LXRα phosphorylation attenuates progression of fatty liver disease. Cell Reports 26:984–995.e6.

[40] Donkin, I., Barrès, R., 2018. Sperm epigenetics and influence of environmental factors. Molecular Metabolism 14:1–11.

[41] Rompala, G.R., Mounier, A., Wolfe, C.M., Lin, Q., Lefterov, I., Homanics, G.E., 2018. Heavy chronic intermittent ethanol exposure alters small noncoding RNAs in mouse sperm and epididymosomes. Frontiers in Genetics 9:32.

[42] Cheong, J.N., Wlodek, M.E., Moritz, K.M., Cuffe, J.S., 2016. Programming of maternal and offspring disease: impact of growth restriction, fetal sex and transmission across generations. Journal of Physiology 594:4727–4740.

[43] Thanh, N.X., Jonsson, E., 2016. Life expectancy of people with fetal alcohol syndrome. Journal of Population Therapeutics and Clinical Pharmacology 23: e53–e59.

[44] Fuglestad, A.J., Boys, C.J., Chang, P.N., Miller, B.S., Eckerle, J.K., Deling, L., et al., 2014. Overweight and obesity among children and adolescents with fetal alcohol spectrum disorders. Alcoholism: Clinical and Experimental Research 38:2502–2508.

[45] Werts, R.L., Van Calcar, S.C., Wargowski, D.S., Smith, S.M., 2014. Inappropriate feeding behaviors and dietary intakes in children with fetal alcohol spectrum disorder or probable prenatal alcohol exposure. Alcoholism: Clinical and Experimental Research 38:871–878.

